

Penta-Coordinated Aluminum Species: New Frontier for Tailoring Acidity-Enhanced Silica- Alumina Catalysts

Zichun Wang,[†] Yijiao Jiang,[†] Alfons Baiker,^{,‡} Jun Huang^{*,§}*

[†] Department of Engineering, Macquarie University, Sydney, New South Wales 2109, Australia

[‡] Institute for Chemical and Bioengineering, Department of Chemistry and Applied Biosciences, ETH Zürich, Hönggerberg, HCI, CH-8093, Switzerland

[§] Laboratory for Catalysis Engineering, School of Chemical and Biomolecular Engineering & Sydney Nano Institute, The University of Sydney, Sydney, NSW 2006, Australia

CONSPECTUS: Silica–alumina catalysts, including zeolites and amorphous silica-aluminas (ASAs), are amongst the most widely used solid acid catalysts and supports to produce petrochemicals, fine chemicals, and renewable energy. The coordination, distribution, and interactions of aluminum in ASAs have an enormous impact on their acidic properties and catalytic performance. Unsaturated tetracoordinated aluminum (Al^{IV}) species are commonly accepted as the key sites in generating catalytically active Brønsted acid sites (BASs) in silica-alumina catalysts. Extensive efforts focus on increasing the concentration of Al^{IV} as the main route to enhance their Brønsted acidity for efficient catalysis. However, increasing the Al^{IV} concentration either weakens the acid strength in zeolites or lowers Brønsted acidity in ASAs at high Al/Si ratios, impeding acidity enhancement of these popular catalysts.

“Penta-coordinated aluminum (Al^{V}) species” are potential unsaturated Al species like Al^{IV} but rarely observed in silica-aluminas, and thus, are widely considered unavailable for BAS formation or surface reactions. In this Account, we will describe novel strategies for the controlled synthesis of Al^{V} -enriched ASAs and corresponding supported metal nanocatalysts using flame spray pyrolysis (FSP) techniques and highlight the contribution of Al^{V} species in acidity enhancement, together with their structure-activity relationship in the conversion of biomass-derived compounds into valuable chemicals. Using various *in situ* and advanced 2D solid-state NMR (SSNMR) experiments, the studies of the acidic properties and local structure of Al^{V} -enriched ASAs reveal that Al^{V} species can highly populate on ASA surfaces, promote BASs formation and facilitate adaptable tuning of BASs from moderate to zeolitic strength by synergy with neighboring Al species. Moreover, the BASs with enhanced acidity can work jointly with surface Lewis acid sites or metal active species for bifunctional catalysis on Al^{V} -enriched ASAs. Compared to zeolites, these Al^{V} -enriched ASAs are highly active in acid-catalyzed biomass conversion, including

alcohol dehydration and sugar conversion reactions, as well as in promoting the performance of supported metal catalysts in chemoselective hydrogenation of aromatic ketones. These new insights provide a state-of-the-art strategy for strongly enhancing the acidity of these popular silica-alumina catalysts, which offers an interesting potential for a wide range of acid and multifunctional catalysis.

KEY REFERENCES

- Wang, Z.; Jiang, Y.; Yi, X.; Zhou, C.; Rawal, A.; Hook, J.; Liu, Z.; Deng, F.; Zheng, A.; Hunger, M.; Baiker, A.; Huang, J. High population and dispersion of pentacoordinated Al^V species on the surface of flame-made amorphous silica-alumina. *Sci. Bull.* **2019**, *64*, 516-523.¹ High population and dispersion of pentacoordinated Al (Al^V) species on the surface of amorphous silica-alumina (ASA) was successfully synthesized for the first time, which is promising to promote surface acidity or act as surface defects for tailoring single-atom catalysts.
- Wang, Z.; Jiang, Y.; Lafon, O.; Trebosc, J.; Kim, K. D.; Stampfl, C.; Baiker, A.; Amoureux, J. P.; Huang, J. Brønsted acid sites based on penta-coordinated aluminum species. *Nat. Commun.* **2016**, *7*, 13820.² A new type of Brønsted acid sites (BASs) based on Al^V was directly observed in ASAs, which could co-exist with BASs formed on tetra-coordinated aluminum sites (Al^{IV}), opening new avenues for strongly enhancing the acidity of ASAs.
- Wang, Z.; Li, T.; Jiang, Y.; Lafon, O.; Liu, Z.; Trébosc, J.; Baiker, A.; Amoureux, J. P.; Huang, J. Acidity enhancement through synergy of penta- and tetra-coordinated aluminum species in amorphous silica networks. *Nat. Commun.* **2020**, *11*, 225.³ A synergistic effect

of two neighboring Al centers interacting with the same silanol group was observed for the first time, which could remarkably increase their acidity for efficient C-H activation and a wide range of acid and multifunctional catalysis.

- Wang, Z.; Jiang, Y.; Jin, F.; Stampfl, C.; Hunger, M.; Baiker, A.; Huang, J. Strongly enhanced acidity and activity of amorphous silica–alumina by formation of pentacoordinated Al^V species. *J. Catal.* **2019**, *372*, 1-7.⁴ Optimizing synthesis conditions by introducing a high flame temperature could promote the formation and distribution of metastable Al^V species in the silica network forming BASs, providing a promising route for the controlled synthesis of Al^V-rich ASAs with higher Brønsted acidity.

1. Introduction

Heterogeneous catalysts dominated the global catalyst market with a revenue of USD 18.0 billion in 2018, motivated by reducing manufacturing costs, emissions, and wastes. Cost-effective alumina and its mixed oxides, amorphous silica-aluminas (ASAs), are among the most popular heterogeneous catalysts and supports for active metal species, extensively used in polymer, chemical, automobile, biorefinery, and petrochemical industries. Their catalytic functions strongly depend on the surface coordination and distribution of Al species and their cooperation with other functional groups and active species.¹⁻⁵ Tetrahedral and octahedral coordination (Al^{IV} and Al^{VI}) are the dominant Al coordinations on alumina and ASAs, however, current efforts in tuning the concentration of Al^{IV} and Al^{VI} species are insufficient for promoting the catalytic activity of alumina and ASAs. Typically, unsaturated Al^{IV} species interacting with neighboring SiOH can contribute catalytically active Brønsted acid sites (BASs), while the Al^{VI} species are associated with introducing Lewis acidity on ASAs. However, increasing the population of Al^{IV} species can significantly reduce the BAS density in ASAs at $\text{Al}/\text{Si} \geq 3/7$,⁶ while $\alpha\text{-Al}_2\text{O}_3$ containing exclusively Al^{VI} species exhibits nearly no Lewis acidity and is catalytically inactive.⁷

Pentahedral coordination (Al^{V}) is a transition coordination between Al^{IV} and Al^{VI} , which recently attracted great interest as a potential candidate for increasing the acidity of alumina and ASAs. Al^{V} species have been identified as defects of Al^{VI} species with an oxygen vacancy,⁸ serving as Lewis acidic sites (LASs) catalyzing versatile reactions (e.g. alcohol dehydration),⁹⁻¹⁰ as well as for anchoring single-metal catalysts (e.g. Ag, Pt, and Pd) to improve their catalytic activity and stability.¹¹⁻¹³ Besides, theoretical calculations have suggested that Al^{V} species could promote BAS formation in ASAs as typically proposed for Al^{IV} .¹⁴ Therefore, increasing the Al^{V} concentration in alumina and ASAs is promising for both enhancing surface Lewis acidity and Brønsted acidity,

thereby overcoming the limitations of current efforts in tuning the concentration of Al^{IV} and Al^{VI} species.

Despite the various potential functions of Al^V species in catalysis, there are still many challenges to be addressed from theory to practice, such as novel approaches for synthesizing Al^V-enriched catalysts and understanding their structure-activity relationship in catalytic reactions. ASAs prepared by conventional wet-chemistry and post-synthetic modification techniques consist mainly of Al^{IV} and Al^{VI} species.¹⁵⁻¹⁷ Al^V species could be generated during phase transformation of γ -alumina to α -alumina under high-temperature calcination (Al^V < 17 at.%),⁷ however, the synthesis of Al^V-enriched ASAs remains difficult. Furthermore, Al^V species are rarely populated on the surfaces of alumina and ASAs,¹⁸⁻¹⁹ even when stabilized by hydroxides and oxides (Al^V < 4 at.%), which impedes Al^V sites to promote catalytic reactions by generating BASs via interaction with surface SiOH groups, and cooperating with other functional groups and active sites for multi-functional catalysis. Therefore, it is technically difficult to characterize the structure, connectivity, and relationship of Al^V species in the presence of other surface species and guest molecules at such low concentrations, hindering the investigation of their intrinsic behavior in promoting the surface acidity of ASAs for efficient catalysis.

This account will describe a new frontier to fabricate acidity-enhanced ASAs based on Al^V species for efficient catalysis and multi-functional catalysis with high efficiency. A novel strategy for tailoring Al^V-enriched ASAs under control by flame-spray pyrolysis (FSP) techniques will be introduced, showing the dominant role and high surface availability of Al^V species through host-guest interaction. First spectroscopic evidence for Al^V promoting BAS formation and significantly enhancing BAS strength through a synergistic effect will be highlighted. Then, detailed structure-acidity-activity correlations of Al^V sites and their cooperation with other functional groups and

active sites of ASAs will be elucidated in various acid-catalyzed reactions on Al^V-enriched ASAs, supported by fruitful state-of-the-art characterization techniques.

2. Al^V species enriched on ASA surface

Flame spray pyrolysis (FSP) techniques are powerful in the synthesis of multi-component nanoparticles dominated by metastable phases and polymorphs²⁰ and thus have been adopted to prepare ASAs enriched with metastable Al^V species. FSP is an emerging one-step method to combine synthesis and calcination of multi-component nanoparticles within milliseconds. When using FSP, Al and Si precursors are homogeneously mixed in a suitable solvent, nebulized by a flow of oxygen, and ignited by an annular methane/oxygen flame for combustion at high temperature (up to 2000 K), followed by fast quenching to room temperature. The oxygen-rich atmosphere and fast cooling rate using FSP is expected to ‘freeze’ metastable species like Al^V species inside the nanoparticles. In contrast, ASAs prepared by wet-chemistry and post-synthetic modification techniques often require high-temperature (ca. 773~1073 K) calcination and a slow cooling rate. The calcination process normally takes hours to days, facilitating atomic rearrangements of Al to thermodynamically stable Al^{IV} and Al^{VI} species, rather than metastable Al^V species in ASAs.

Using FSP, Al^V-enriched ASAs are successfully synthesized using e.g. methanol/acetic acid (1:1 by volume) mixture as solvent/fuel,⁵ designating as SA/*X*, where *X* represents the atom% of Al in the precursor. ²⁷Al multiple quantum MAS (MQMAS) experiments are commonly used to determine the coordination and the local asymmetry of Al nucleus,²¹ by which, dominant Al^V and Al^{IV} species with trace Al^{VI} species in dehydrated SA/*X* catalysts are observed (Fig. 1a and 1c). Their concentrations are determined by simulating corresponding 1D ²⁷Al NMR spectra using quadrupole parameters obtained in ²⁷Al MQMAS experiments as exemplified in Table 1. Al^V

species are often reported to be associated with Al^{VI} species in alumina or at interfaces between alumina and mixed silica-alumina phases in ASAs.^{7, 22} The absence of Al^{VI} species indicates that the formation Al^V species is virtually independent of the alumina phase in flame-derived ASAs, as supported by an XRD amorphous and alumina-free lattice structure in HRTEM.¹

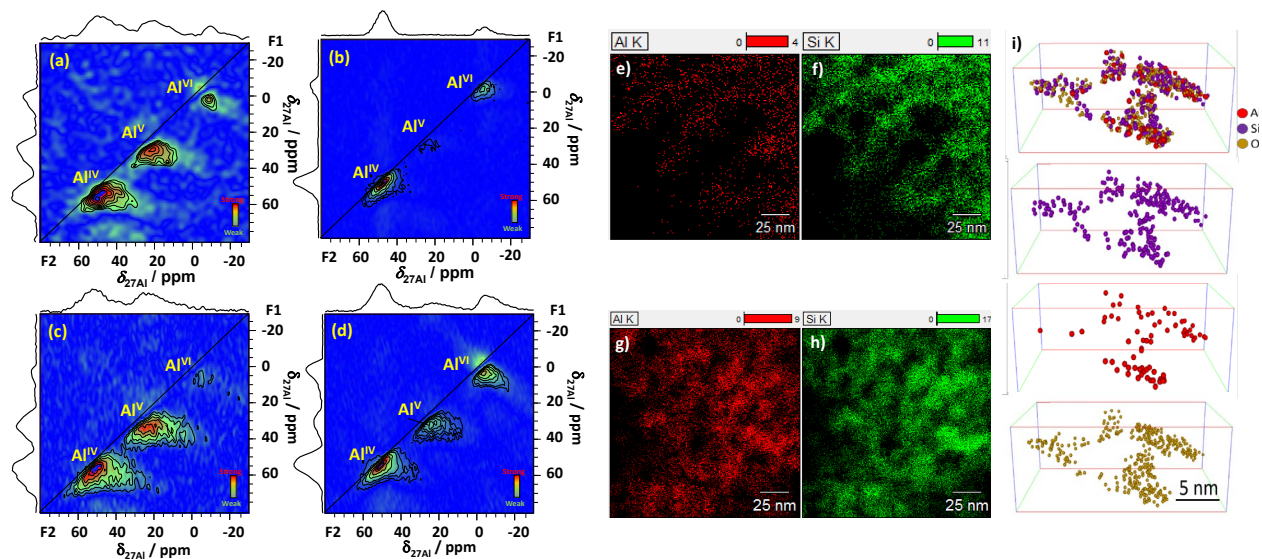


Figure 1. ²⁷Al MQMAS NMR spectra of SA/10 (a, b) and SA/30 (c, d) after dehydrated at 723 K (a, c) and after rehydration (b, d), recorded at a magnetic field of 16.4 T. EDX images of SA/10 (e, f) and SA/30 (g, h). Reproduced with permission from ref. 1. Copyright 2019 Elsevier. (i) 3D-APT reconstruction of isolated SA/10 nanoparticles. Reproduced with permission from ref. 3. Copyright 2020 Nature Research.

Table 1. Al concentration and population density of BASs in Al^V-enriched ASAs. Reproduced with permission from ref. 4. Copyright 2019 Elsevier and ref. 5 Copyright 2010 Wiley.

	Al ^{IV} (at.%)	Al ^V (at.%)	Al ^{VI} (at.%)	BAS density (mmol/g)
SA/10	62	37	1	9.8×10 ⁻²
SA/30	51	48	1	11.1×10 ⁻²

SA/50	42	51	7	13.4×10^{-2}
SA/70	41	55	4	15.1×10^{-2}

Surface Al species could be identified through host-guest interaction using pertinent probe molecules. Upon water adsorption, partial hydrolysis of surface Al^{IV} species to Al^{VI} species is often observed in zeolites and ASAs,²³⁻²⁴ as well as strong reduction of the local asymmetry of Al species.^{18, 24} The high surface availability of Al^V species in ASAs is demonstrated by converting most Al^V species (up to 34.7 at.%) into Al^{VI} species upon rehydration (Fig. 1b and 1d).

Unsaturated surface Al species distributed in the silica network could enhance the acid strength of neighboring SiOH groups in ASAs, as typically proposed for Al^{IV} species. In Al^V-enriched ASAs, EDX atom mapping (Fig. 1e-h) and the reconstruction of the 3D structure by atom probe tomography (APT, Fig. 1i) shows that Al species are homogeneously distributed into the silica network,^{1, 3} which is further supported by a systematic change of the ²⁹Si NMR signal with increasing Al addition.⁴⁻⁵ Therefore, the Al^V species highly populated on ASA surfaces exhibit a high predisposition to interact with surface SiOH groups, which are promising BASs as proposed in DFT calculations.¹⁴

3. Brønsted acid sites formed based on Al^V species

Al^V species interacting with surface SiOH groups are considered to be BASs, however, identifying the interaction between Al species with different coordinations and surface SiOH groups in ASAs is rather demanding. Conventional ²⁷Al magic-angle spinning (MAS) 1D SSNMR techniques, such as ¹H/²⁷Al transfer of population in double resonance (TRAPDOR) and ²⁷Al{¹H} cross-polarization MAS experiments, could probe OH groups with neighboring Al sites without

distinguishing their coordination.²⁵ Various advanced two-dimensional (2D) SSNMR experiments are employed to determine the composition, structure, connectivity, and correlations between Al species and/or protons with other probe molecules on zeolites.²⁶⁻²⁷ However, their applications in the study of ASAs is quite challenging due to the signal of low sensitivity and strong overlapping, caused by the absence of long-range ordering of the constituents and wide coordination distribution of Al species. In terms of the dispensable role of Al^V species in conventional ASAs, the detection of BASs formed on Al^V species is unachievable.

Using Al^V-enriched ASAs provides a great chance to investigate the correlations between Al^V species and surface functional groups, such as BASs generated by Al^V species having neighboring SiOH groups. ²⁷Al-¹H} dipolar-mediated heteronuclear multiple quantum correlation (D-HMQC) 2D NMR experiments at high magnetic field (18.8 T) enable detecting ¹H via ²⁷Al nuclei. It shows that Al^{IV} species pseudo-bridging to neighboring silanol oxygen (Fig. 2a) can enhance their acid strength to protonate ammonia (Fig. 2b), acting as BAS (Al^{IV}-BAS). Similar behavior is observed with Al^V species demonstrating connectivity between Al^V species and SiOH groups, thereby contributing Al^V-BASs (Fig. 2). In contrast to the general knowledge about Al^{IV}-rich ASAs, the BAS density shows an inverse correlation to the Al^{IV} concentration in Al^V-enriched ASAs but it correlates well to the increase of the Al^V concentration (cf. Table 1). This observation indicates that the BAS density in ASAs can be promoted by the co-existence of Al^V and Al^{IV} species, other than replacing each other to reduce BAS density.

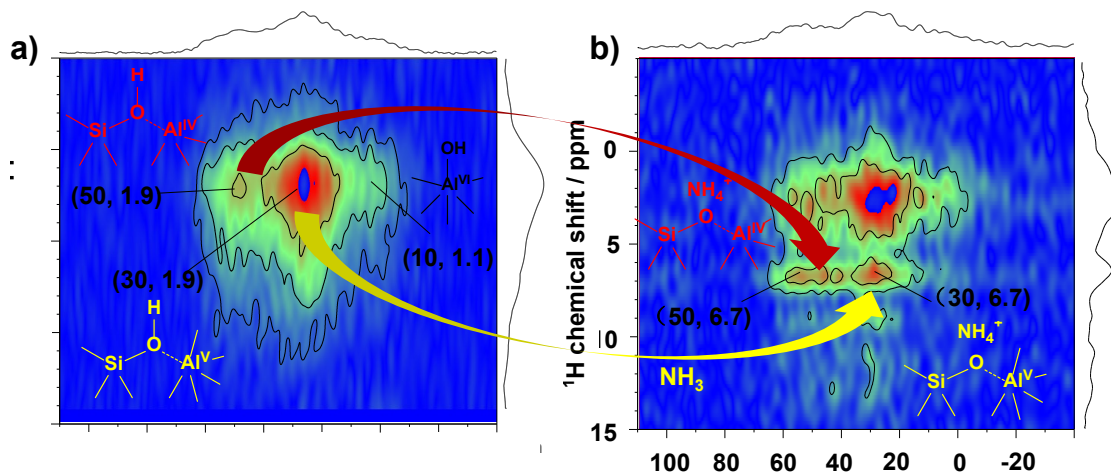


Figure 2. $^{27}\text{Al}\{-^1\text{H}\}$ D-HMQC 2D spectrum of SA/50. (a) SA/50 dehydrated at 723 K for 12 h under vacuum, and (b) after ammonia loading and evacuated at 373 K for 1 h. The spectra were recorded at 18.8 T with a MAS frequency of $\nu_{\text{R}} = 20$ kHz and $\tau_{\text{rec}} = 1.0$ ms for dehydrated and $\tau_{\text{rec}} = 900$ μs for ammonia-loaded sample, respectively. Reproduced with permission from ref. 2. Copyright 2016 Nature Publishing Group.

To gain deeper insight into candidate structures of Al^{V} -BAS, density functional theory (DFT) and simulation studies were done.^{1, 28} The structure information of the optimized models derived from DFT calculations are in line with those obtained from SSNMR experiments. Al^{V} species correlating to neighboring SiOH groups in dehydrated state have been confirmed in Fig. 3a and 3c. The surface availability of Al^{V} species is demonstrated by coordination transfer to either Al^{IV} (Fig. 3b) or Al^{VI} species (Fig. 3d and 3f) upon rehydration. Moreover, surface Al^{V} species as part of small Al clusters in Al^{V} -enriched ASAs are observed as well (Fig. 3e and 3f). These species are potential LASs as revealed by temperature-programmed desorption of ammonia-loaded Al^{V} -enriched ASAs.²⁹ Moreover, $^{17}\text{O}\{^1\text{H}, ^{27}\text{Al}\}$ resonance-echo saturation pulse double-resonance (RESPDOR) TRAPDOR experiments have been developed to determine the Al-OH distance by

measuring the $^{17}\text{O}\{^{27}\text{Al}\}$ TRAPDOR dephasing curves of hydroxyl oxygen²⁸ These experiments facilitate discriminating the structure of Al^{V} -BASs from two possible candidates, such as bridging OH groups (1.88–2.0 Å) and PBS (Pseudo-Bridging Silanol, 2.94–4.43 Å).¹⁴ Combining the experimental data with simulation curves demonstrates that the PBS model is the most feasible for BASs generated in Al^{V} -enriched ASAs, for both Al^{V} -BASs and Al^{IV} -BASs (Fig. 3g).

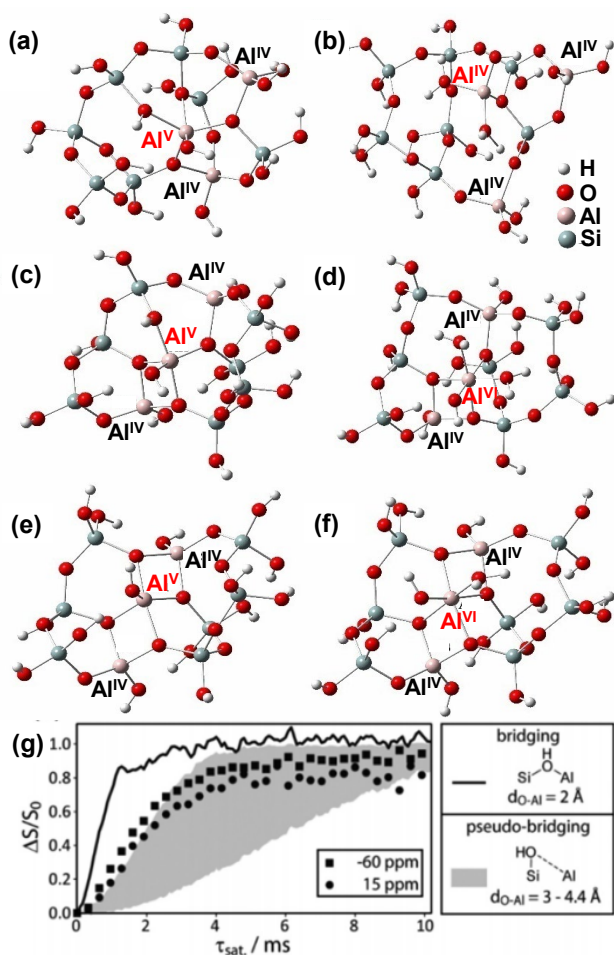


Figure 3. Optimized structure of Al^{V} species in dehydrated states (a, c and e) and in corresponding rehydrated states (b, d, and f), both calculated at B3LYP/6-31g (d) theoretical level. Reproduced with permission from ref. 1. Copyright 2019 Elsevier. (g) $^{17}\text{O}\{^{27}\text{Al}\}$ TRAPDOR curves obtained from $^{17}\text{O}\{^1\text{H}, ^{27}\text{Al}\}$ RESPDOR-TRAPDOR experiment were simulated to determine the Al-OH

distance, for discriminating the structure of Al^V-BASs, corresponding to bridging silanols (black line, O–Al distance of 2 Å) and pseudo-bridging silanols (gray shaded area, O–Al distance range of 3 to 4.4 Å). Reproduced with permission from ref. 28. Copyright 2019 Royal Society of Chemistry.

4. Strong BAS generated by the synergy of nearby Al species

Besides promoting BASs formation in ASAs, increasing the BAS strength is a more challenging task to enhance their catalytic activity for various applications. In general, the acid strength of solid acids can be scaled using 2-¹³C-acetone as a probe molecule because a larger low-field shift of the ¹³C NMR signal hints to higher acid strength. In classic Al^{IV}-rich ASAs, exclusively moderate Al^{IV}-BASs with a signal at $\delta_{13C} = 213\text{-}215$ ppm are commonly probed,³⁰⁻³¹ much weaker compared to bridging OH groups in zeolites ($\delta_{13C} = 216\text{-}225$ ppm).³² Although Al^{IV}-BASs and Al^V-BASs are co-existing in Al^V-enriched ASAs in SA/10, mainly moderate BASs can be detected (Fig. 4), hinting to similar acidic properties and structure of Al^{IV}-BASs and Al^V-BASs. So far, all models proposed for Al^{IV}-BASs and Al^V-BASs are based on one Al^{IV} or Al^V center interacting with a SiOH group,² providing mainly moderate BAS strength, much weaker than BASs in zeolites.

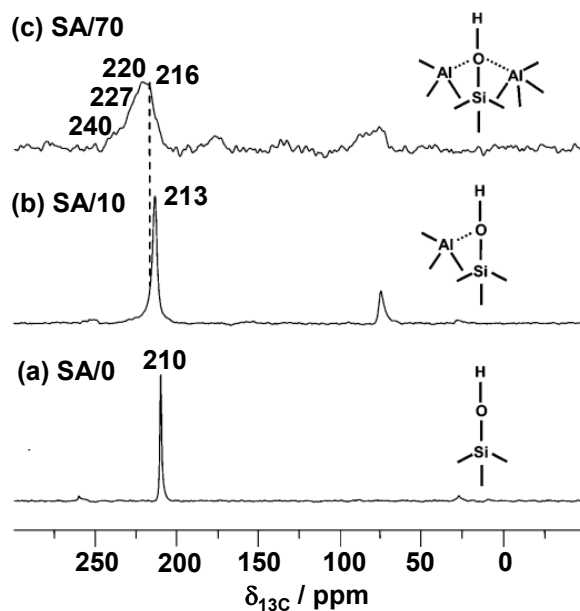


Figure 4. ^{13}C MAS NMR spectra of acetone- $2\text{-}^{13}\text{C}$ -loaded Al^{V} -enriched ASAs. Reproduced with permission from ref. 5. Copyright 2010 Wiley.

Evaluating the acid strength in Al^{V} -enriched ASAs demonstrates that BAS with zeolitic strength ($\delta_{13\text{C}} = 220\text{-}227$ ppm) are generated in Al^{V} -enriched ASAs at high Al/Si ratios (Fig. 4c).⁵ Since the formation of zeolitic bridging OH groups is unfavorable in ASAs, exploring the novel structure experimentally and theoretically, is highly desired for developing strong BASs in ASAs.^{14, 28} FSP provides a homogeneous distribution of aluminum atoms in the silica network at low Al/Si ratio (Fig. 1e-i), while silicon atoms are highly dispersed throughout an alumina-rich matrix at high Al/Si ratio, showing that more than one Al center could be in proximity to the same silicon atom (Fig. 5a-e). The ^{27}Al DQ-SQ 2D NMR spectrum of dehydrated SA/50 (Fig. 5f-k) is dominated by strong correlations between Al species, such as $\text{Al}^{\text{IV}}\text{-Al}^{\text{V}}$ and $\text{Al}^{\text{V}}\text{-Al}^{\text{V}}$, while no obvious correlation between Al spins can be detected in dehydrated SA/10. In ASAs, a stronger polarization on the silanol oxygen by neighboring Al center(s) leads to a higher acid strength of the silanol proton. Since those strong correlations of Al species are independent of the formation

of an alumina phase, there is a high probability that they exist in the local structure of silanols. In terms of the significantly higher BAS strength in SA/50 than in SA/10, these strong correlations are proposed to promote BASs with zeolitic strength (Fig. 6a and 6b).

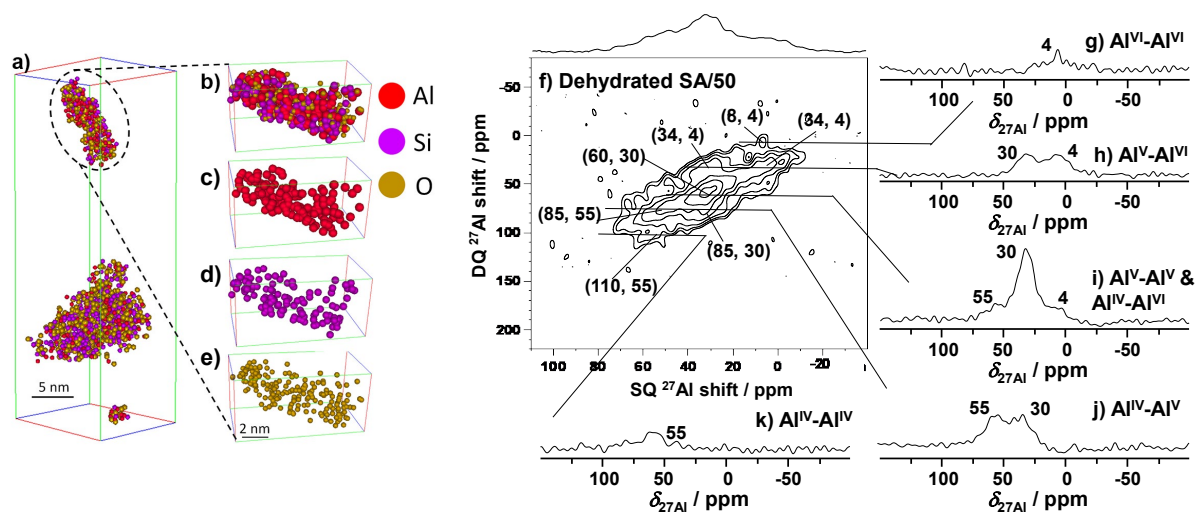


Figure 5. (a-e) 3D-APT reconstruction of two isolated SA/50 nanoparticles showing all atoms. (f) ^{27}Al DQ-SQ 2D NMR spectrum recorded at 18.8 T with $\nu_R = 20$ kHz of dehydrated SA/50. (g-k) Rows extracted from the 2D spectrum corresponding to the various autocorrelation and cross-peaks. Reproduced with permission from ref. 3. Copyright 2020 Nature Research.

A pseudo ‘oxygen tri- or tetra-cluster’ model (Fig. 6b) has been proposed to account for the strong BAS generated in Al^{V} -enriched ASAs. An extra Al center pseudo-bounded to the same silanol could further polarize the silanol oxygen, and thus, enhance the BAS strength from weak to strong. This is similar to the situation reported for zeolites where the strength of bridging OH groups can be further enhanced through an electron density withdrawing effect by neighboring extra-framework Al species through a Brønsted/Lewis acid synergy.³³ The formation of oxygen tri- or tetra-cluster are proposed for aluminosilicate glasses, and ASAs prepared by SiO_2 grafted on Al_2O_3 supports, driven by the increasing ionicity at high Al/Si ratio.^{17, 34} Since the deposition

of organosilanes is based on their selective reaction with surface AlOH groups, including Al-OH-Al groups, these works only focus on the Si atoms of the silanols bridging to Al-O-Al groups on Al₂O₃ supports, other than the silanol oxygen. In these models, neighboring unsaturated Al centers are scarce for stabilizing the silanolate formed after deprotonation of acidic SiOH groups, and thus, are less effective in promoting surface Brønsted acidity.

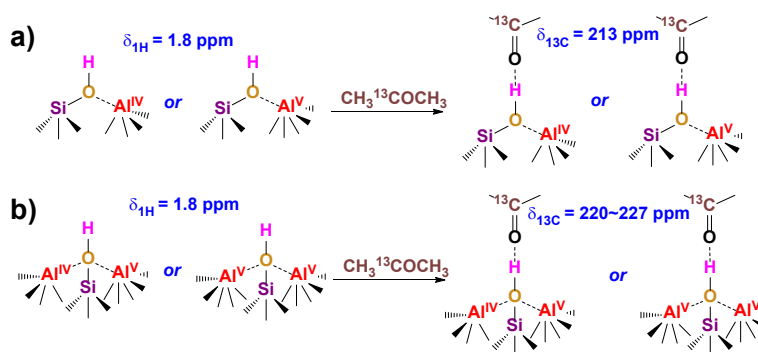


Figure 6. Proposed models for BAS on ASAs generated by: (a) one Al center per SiOH for moderate BAS, and (b) two Al centers per SiOH group, leading to zeolitic acid strengths. Reproduced with permission from ref. 3. Copyright 2020 Nature Research.

5. Structure–activity correlations study

5.1. C-H activation over acidity-enhanced Al^V-enriched ASAs

Activation of C-H bonds over solid acids is a key step in industrial hydrocarbon conversion processes, such as (hydro-)cracking, alkylation, isomerization, and dehydrogenation reactions. Strong BASs could facilitate proton transfer to activate hydrocarbon molecules. As an example, zeolites having strong BASs are effective in the C-H bond activation of benzene promoting the alkylation processes of aromatic compounds.³⁵⁻³⁸ *In situ* ¹H SSNMR demonstrates that H/D exchange is mainly occurring at bridging OH groups ($\delta_{1H} = 4$ ppm) in zeolite H-ZSM-5, which

significantly decreases with the compensation of a signal at $\delta_{\text{IH}} = \text{ca. } 7.5 \text{ ppm}$ by hydrogen bound to aromatic rings (Fig. 7a).

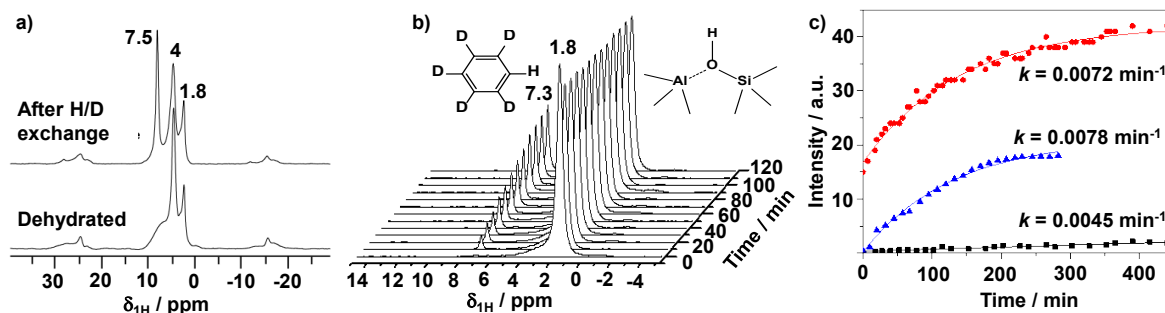


Figure 7. Catalytic performance of H-ZSM-5 and Al^{V} -enriched ASA in H/D exchange with d_6 -benzene at 313 K. ^1H MAS spectra at 9.4 T of (a) Zeolite H-ZSM-5 and (b) stack plot spectra of SA/50. (c) Kinetics and H/D exchange rates k for ZSM-5 (top), SA/50 (middle), and SA/10 (bottom). Reproduced with permission from ref. 3. Copyright 2020 Nature Research.

The remarkable enhancement of the Brønsted acidity in Al^{V} -enriched ASAs could increase their activity in hydrocarbon conversion via C-H bond activation.^{2, 5} Using SA/50, the systematic decrease of the signal at $\delta_{\text{IH}} = 1.8 \text{ ppm}$ with increasing the signal at $\delta_{\text{IH}} = 7.3 \text{ ppm}$ indicates that the H/D exchange occurs at acidic SiOH groups (Fig. 6) on the ASA. Often, a higher H/D exchange rate k indicates a higher BAS strength, where k is determined by fitting corresponding kinetic data. A slightly higher k value was obtained with SA/50 than with H-ZSM-5 zeolite, and both values are much higher than that achieved with SA/10, indicating that the BAS strength increased in the order of $\text{SA/10} \ll \text{H-ZSM-5} < \text{SA/50}$, in line with ^{13}C MAS NMR studies.⁵ Clearly, the synergy of more than one Al center inside silica networks can generate BAS with zeolitic strength and is therefore of great potential for enhancing the activity of ASAs for C-H activation reactions.

5.2. Acidity enhancement and efficient biomass conversion using Al^{V} -enriched ASAs

Green and sustainable chemical production from biomass-derived compounds is desirable to replace those produced from fossil feedstocks. Zeolites are extensively utilized in the conversion of hydrocarbons from fossil feedstocks and in biomass conversion reactions. However, biomass reactions often involve reactions of large molecules, resulting in mass transfer issues inside the small pores and channels of zeolites.³⁹

Nonporous ASAs provide virtually unconstrained diffusion of reactants/products to and from surface sites and are thus of great interest for biomass conversions. For example, dealuminated HY (De-Al-HY) zeolites are considered as the most active solid acids in the production of alkyl mandelates via redox disproportionative conversion of aromatic aldehydes such as phenylglyoxal (PG),⁴⁰ which are important chiral building blocks in the synthesis of pharmaceuticals and fine chemicals.⁴¹ In general, strong BASs can activate reactant molecules for catalytic reaction more efficiently than moderate BASs. Higher turnover frequency (TOF) indicates higher activity of surface sites. However, ASAs ($\text{Si/Al} \leq 30\%$) consisting of moderate BASs afford up to 20 times higher TOFs than De-Al-HY with strong BASs (Table 2), which is attributed to the rapid adsorption/removal of reactants/products from the surface sites. SA/70 with enhanced BAS density and strength provided a 16% higher EM yield than De-Al-HY at the same reaction conditions. The higher activity of SA/70 has been further confirmed by PG conversion in *i*-propanol and showed generally excellent performance in various alkyl alcohols (Fig. 8a). This example indicates that the free surface diffusion of large molecules together with enhanced acidity are keys to the superior performance of ASAs.

Table 2. Catalytic data of PG conversion to ethyl mandelate over ASAs and De-Al-HY. Reproduced with permission from ref. 42. Copyright 2013 American Chemical Society.

Catalyst	A_{BET}^a	Y_{EM}^b	S_{EM}^c	BAS ^d	LAS ^d	TOFs ^e
----------	--------------------	-------------------	-------------------	------------------	------------------	-------------------

	m ² /g	(%)	(%)	mmol/g	mmol/g	(h ⁻¹)
SA/0	156	0	0	0	0	0
SA/10	377	56	93	0.098	0	10.2
SA/30	248	67	94	0.111	0	10.5
SA/50	222	81	95	0.134	0.003	10.5
SA/70	200	97	97	0.151	0.008	10.5
De-Al-HY ³⁵	671	81	90	0.865	1.75	0.57

^a The surface areas (A_{BET}) of SAs were taken from ref. (8). ^b Y_{EM} = yield of ethyl mandelate in mol%. ^c S_{EM} = selectivity to ethyl mandelate at 50% conversion. ^d Densities of BASs and LASs of ASAs and De-Al-HY are depicted from ref. ⁵ and ref. ³⁵, respectively. ^e TOFs were calculated based on the conversion after 6 h reaction, including both BASs and LASs.

Besides acidity enhancement and free mass transfer, biomass conversion on ASAs often involves multiple acid-catalyzed reaction steps. Bifunctional Brønsted-Lewis acid catalysts could promote reactions through the concerted action of both sites or via cascade reactions.⁴³⁻⁴⁵ Bifunctional Brønsted-Lewis acidic zeolites are typically prepared by framework dealumination or Al exchange to introduce Lewis acidic extra-framework Al (EFAl) species.^{33, 46} However, these species can easily leach out in liquid-phase reactions, resulting in severe activity loss.^{3, 47} As an example, the concerted action of BAS and LAS is proposed for the efficient conversion of glyceraldehyde to alkyl lactates, however, the reuse of De-Al-HY causes a severe drop in activity and selectivity, while SA/50 exhibits similar activity before and after reuse under the same conditions (Fig. 8b). The high stability of Al^V-enriched ASAs are also retained after steam

treatment (433 K) and high-temperature calcination (1073 K), and thus, they are interesting for applications in various gas-phase reactions as well.

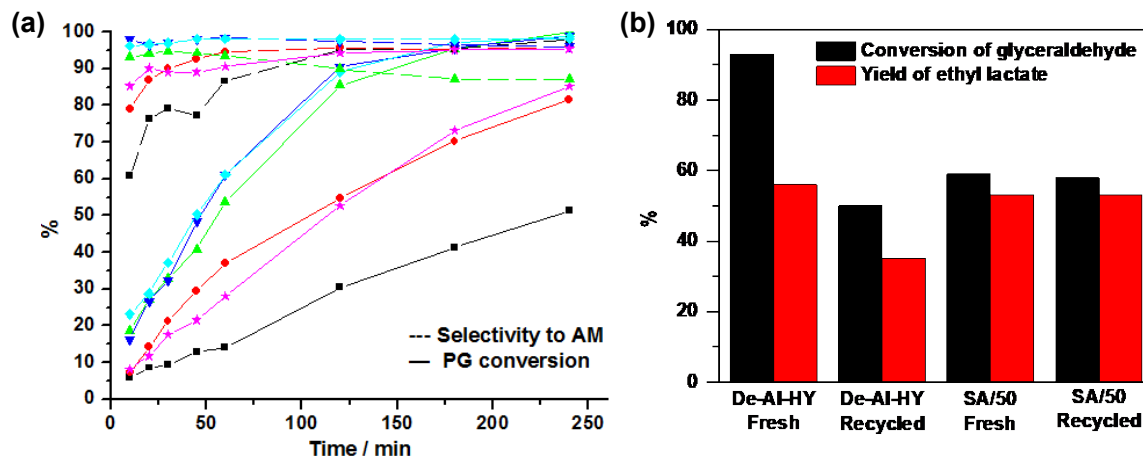


Figure 8. Catalytic conversion of C3 sugars over ASAs. (a) Catalytic conversion of phenylglyoxal (—) and selectivity to alkyl mandelate (---) as a function of reaction time in MeOH (■), EtOH (●), i-PrOH (▼), n-PrOH (◆), n-BuOH (▲), and reaction in i-PrOH (★) over De-Al-HY. Reproduced with permission from ref. 42. Copyright 2013 American Chemical Society. (b) Catalytic glyceraldehyde conversion in ethanol over fresh De-Al-HY and SA/50 and after five recycle uses. Reproduced with permission from ref. 3. Copyright 2020 Nature Research. Conditions: 1.25 ml of alcohol solution containing 0.4 M phenylglyoxal or glyceraldehyde, 0.05 g catalyst, at 363 K for 6 h with stirring.

The high stability of Al^V-enriched ASAs is also confirmed (Table 3 last row) in the catalytic conversion of glucose to 5-hydroxymethylfurfural (HMF), which is a valuable building block in the production of liquid alkanes, biofuels, and furan derivatives.⁴¹ Glucose dehydration to HMF often requires glucose isomerization at LASs to fructose, which subsequently undergoes dehydration to HMF at BASs. The homogeneous distribution of Al^V species mainly contributes to the generation of surface BASs in SA/10 but provides a limited potential for forming LASs,

leading to a lower performance than ASAs prepared by classical techniques (Table 3 row 3-5), though the former possesses much higher BAS density. SA/50 provides excellent performance among these silica-alumina catalysts, even better than bifunctional Fe-ZSM-5 zeolite, requiring a shorter reaction time and lower reaction temperature. As demonstrated in Fig. 1 and 5, an increasing number of Al^V species at high Al/Si could either promote LAS formation or enhance BAS strength via Al^V and Al^{IV} synergy. The concerted action of enhanced LASs and BASs in SA/50 can promote both glucose isomerization and fructose dehydration efficiently. Therefore, the synergy of Lewis acidic Al^V and enhanced Brønsted acidity render Al^V-enriched ASAs excellent bifunctional Brønsted-Lewis acid catalysts for glucose dehydration and potential applications in the conversion of other hexoses and glucose-based carbohydrates, including sucrose, cellobiose, starch, and cellulose under the same conditions.

Table 3. Catalytic performance of ASAs and pertinent reference catalysts in the conversion of glucose to HMF.^a Reproduced with permission from ref. 3. Copyright 2020 Nature Research.

	Temp (K)	Time (h)	Conversion (%)	Yield (%)	Ref.
Fe-ZSM-5, Si/Al = 22.8 ^b	468	2.5	90	33	48
ASA ^c , Si/Al = 90/10	433	2	45	18.8	This work
SA/10, Si/Al = 90/10	433	2	23	6.3	
SA/50, Si/Al = 50/50	433	2	70 (68)	38 (37) ^d	

^a Conditions: catalyst (0.02 g) was added to a mixture of deionized water (0.6 mL) and DMSO (1.4 mL) containing glucose (0.06 g). ^b Conditions: catalyst (0.05 g) was added to a mixture of deionized water (1.5 mL) and MIBK (3.5 mL) containing glucose (0.15 g). Fe/Al = 0.21. ^c ASA prepared by co-precipitation. ^d The catalytic data after five recycle runs are given in parentheses.

6. Optimizing FSP conditions for tailoring high-performance ASAs

Taking the versatile advantages described above, enriching the concentration of Al^V species in ASAs is desirable through optimizing FSP conditions. Al^V species can be generated under conditions of extremely high temperature, an oxygen-rich atmosphere, and a fast cooling rate. The temperature and concentration profiles as well as the residence time of the individual component and cooling rates have a critical influence on the final properties of FSP-derived materials. The temperature profile, which establishes in the FSP reactor strongly depends on the heat generated by the combustion of the solvent used for the precursors. As an example, xylene provides a higher combustion enthalpy (36.9 kJ/ml) than a methanol/acetic acid (Me/AA) mixture (volume ratio 1/1) with a combustion heat of ≈ 25.4 kJ/ml. In the following, FSP ASAs prepared using xylene are designated as SA/ Xx , where X represents the Al concentration (at%) in the precursor, and x stands for xylene used as the solvent.

Feeding the flame with xylene as the precursor solvent generates a higher flame temperature with a faster cooling rate under the same conditions, and consequently, enhances the freezing of metastable Al^V species in FSP ASAs (Fig. 9a).⁴ The higher Al^V population provides more connections between Al^V species and neighboring SiOH groups, and thus, the Al^V concentration-dependent BAS formation increased by up to 30% using xylene compared to using Me/AA as solvent. Compared to Al^{IV} -rich ASAs, SA/ Xx catalysts exhibit up to an order of magnitude higher BAS densities.⁴⁹ Moreover, SA/ Xx catalysts exhibit comparable BAS density at significantly lower Al content than SA/ X catalysts (e.g. SA/30x and SA/70). It shows that using a solvent with higher combustion enthalpy (e.g. xylene) does not only increase the Al^V concentration but can also promote the distribution of Al species over the silica network and thus the formation of BASs. Therefore, this approach provides a potential way for the synthesis of ASA materials with higher acidity at lower Al content.

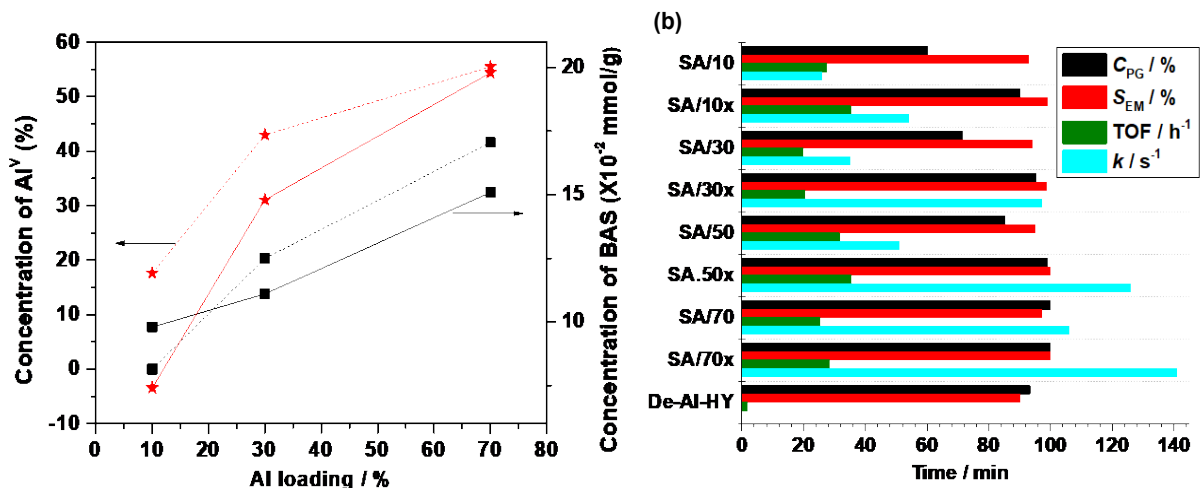


Figure 9. (a) Correlation between the concentration of Brønsted acidic OH groups (BAS, solid line) and Al^V species (dashed line) as a function of the Al content in dehydrated FSP SAs prepared by using methanol/acetic acid (1:1 by volume) (■) and xylene (★), respectively. (b) Catalytic conversion of PG in ethanol. and are The PG conversion (C_{PG}), EM selectivity (S_{EM}), reaction rates k , and TOFs were obtained from ref. 4, respectively. Same reaction conditions as shown in Fig. 8.. Reproduced with permission from ref. 4. Copyright 2019 Elsevier.

The catalytic performance of Al^V-enriched ASAs prepared by using xylene was evaluated in PG conversion with ethanol, and compared to that achieved with corresponding ASAs prepared using Me/AA (Fig. 9b). Significantly higher PG conversion and EM selectivity were attained using SA/*Xx* instead of SA/*X* catalysts. The increasing Al^V concentration achieved with xylene could promote BAS formation with both high density and strength. The higher TOFs obtained at the initial state show that the individual sites on SA/*Xx* are highly active compared to those on SA/*X* catalysts because the enhanced Brønsted acidity facilitates the activation of the C=O bond in PG as the initiating step.⁵⁰ The enhanced acidity promoted the reaction rate k of the PG conversion by 1.3-2.8 times at the same level of Al addition, and SA/70x is considered as the most active solid acid catalyst for this reaction hitherto. Moreover, SA/*Xx* catalysts afford a similar PG conversion

and k value as SA/ X catalysts with higher Al addition, which is of great potential for synthesizing high-performance ASA materials with lower Al addition.

7. Conclusions and outlook

ASAs without diffusional constraints exhibit superior catalytic performance compared to zeolites in reactions with large molecules, such as encountered in biomass conversions. However, the moderate acid strength of BASs of most ASAs impedes improving their catalytic performance and expanding their applications compared to zeolites with strong BASs. Enhancing Brønsted acidity in ASAs is hindered by the classic theory that BAS formation is based on Al^{IV} species interacting with neighboring SiOH groups affording only moderate BAS strength. Extensive efforts are still devoted to increasing the BAS density by tuning the Al^{IV} concentration but this strategy is limited by significant self-condensation of Al^{IV} species (Al-O-Al), replacing Al-O-Si connections at Al/Si ratios $> 3/7$. Therefore, the discovery of new BASs in ASAs by theoretical innovation has attracted great attention, aiming at developing novel strategies to enhance the acidity in ASAs for efficient biomass conversions.

Al^V species are proposed to exhibit similar properties as Al^{IV} species but are rarely observed in ASAs prepared hitherto. Bridging the assumption and synthesis, a novel strategy based on flame-spray pyrolysis has been developed for the controlled synthesis of Al^V -enriched ASAs ($37\% < Al^V < 61\%$). Through the application of various characterization techniques combined with theoretical studies, two new types of BASs based on Al^V sites and the interaction of two Al sites (e.g. Al^V and Al^{IV}) with the same SiOH group were uncovered. Experimental and theoretical studies on their structure-acidity relationship demonstrate that the former Al^V -BASs exhibit moderate strength like typical Al^{IV} -BASs in ASAs, while the latter afford BASs with zeolitic

strength. The co-existence of Al^{V} and Al^{IV} can promote BASs formation in Al^{V} -enriched ASAs with a density 10 times higher than those obtained with Al^{IV} -rich ASAs. Besides contributing to Al^{V} -BASs, Al^{V} sites are observed to act as LASs upon ammonia adsorption. Together with LASs, the flexible tuning of BASs from moderate to strong with higher BAS density significantly enhances the catalytic performance of Al^{V} -enriched ASAs in both single- and bi-functional acid-catalytic reactions, such as C-H activation of benzene, sugar conversions, and redox disproportionative conversion of aromatic aldehydes.

Despite the strong acidity and excellent performance of Al^{V} -enriched ASAs, a strategy for synthesizing Al^{V} -enriched ASAs at milder conditions, e.g. by improved wet-chemistry routes, is desired to expand their industrial applications without practical limitations for scale up. Moreover, unsaturated Al^{V} sites have been already identified as key sites for anchoring single-atom catalysts on alumina, compared to other Al species.⁵¹ Single-atom catalysts have shown excellent performance in a wide range of applications, such as water-gas-shift reactions, reforming reactions, CO oxidation, organic reactions, and de NO_x reactions.⁵²⁻⁵³ Since Al^{V} species are populated on the surface of Al^{V} -enriched ASAs, they are potential supports for tailoring single-atom catalysts. Combining the strongly enhanced acidity on Al^{V} -enriched ASAs, the synergy between atomic metal active sites and acid sites facilitates the design of promising multifunctional catalysts for versatile catalytic applications, such as chemoselective hydrogenation and oxidation reactions.

AUTHOR INFORMATION

Corresponding Author

*E-mail: (J.H.) jun.huang@sydney.edu.au

*E-mail: (A.B.) alfons.baiker@chem.ethz.ch

Author Contributions

The manuscript was written through contributions of all authors. All authors have approved the final version of the manuscript.

Notes

The authors declare no competing financial interest.

Biographies

Zichun Wang received his Ph.D. degree (2015) from the University of Sydney. After three years postdoctoral researches, he joined Macquarie University (Australia) and currently an Australia Research Council Discovery Early Career Research Award fellow. His research focuses on rational design of heterogeneous catalysts for green and sustainable energy and chemical production, through in situ spectroscopic studies on catalyst structure and reaction mechanism.

Yijiao Jiang received her Ph.D. in Chemical Technology from the University of Stuttgart in 2007. She worked as postdoc at ETH Zürich from 2008 to 2010. She held an UNSW Vice-Chancellor's Research Fellowship in 2011 and ARC Discovery Early Career Researcher Award between 2012 and 2014. She then joined the Macquarie University and became Associate Professor in 2020. Her research interests mainly focus on the development of better catalytic systems and various operando spectroscopic techniques for green chemical processes, renewable energy production and environmental protection.

Alfons Baiker studied chemical engineering at ETH Zurich and earned his Ph.D degree in 1974. After several postdoctoral stays at various universities, he returned from Stanford University (California) to ETH, setting up his research group and stepped up the ranks to become Full Professor in 1990. His research interests, documented in over 900 publications in refereed journals

and numerous patents, are centered on catalyst design and novel catalytic materials, mechanisms and kinetics of catalytic surface processes, chiral surfaces, asymmetric hydrogenation, selective oxidation, environmental catalysis, operando spectroscopy, and the application of supercritical fluids in catalysis.

Jun Huang received his PhD from University of Stuttgart in 2008. After his postdoctoral fellow at Georgia Institute of Technology and ETH, he joined the University of Sydney as a permanent faculty in 2010, starting his research group focusing on catalysis engineering and in situ characterization, moving up the ranks to Associate Professor at Sydney. His research is to develop emerging catalytic technologies for more attractive, practical, and cleaner processes using in situ characterization techniques, coupled with new catalyst design and innovative reaction engineering.

ACKNOWLEDGMENT

J.H. and Z.W. acknowledge the financial supports from Australian Research Council Discovery Projects (DP150103842, DP180104010, and DE190101618). J.H. thanks the University of Sydney SOAR fellowship, Sydney Nano Grand Challenge, and the International Project Development Funding.

REFERENCES

- (1) Wang, Z.; Jiang, Y.; Yi, X.; Zhou, C.; Rawal, A.; Hook, J.; Liu, Z.; Deng, F.; Zheng, A.; Hunger, M.; Baiker, A.; Huang, J. High population and dispersion of pentacoordinated Al^V species on the surface of flame-made amorphous silica-alumina. *Sci. Bull.* **2019**, *64*, 516-523.
- (2) Wang, Z.; Jiang, Y.; Lafon, O.; Trebosc, J.; Kim, K. D.; Stampfl, C.; Baiker, A.; Amoureux, J. P.; Huang, J. Brønsted acid sites based on penta-coordinated aluminum species. *Nat. Commun.* **2016**, *7*, 13820. DOI: 10.1038/ncomms13820.

- (3) Wang, Z.; Li, T.; Jiang, Y.; Lafon, O.; Liu, Z.; Trébosc, J.; Baiker, A.; Amoureux, J. P.; Huang, J. Acidity enhancement through synergy of penta- and tetra-coordinated aluminum species in amorphous silica networks. *Nat. Commun.* **2020**, *11*, 225, DOI: 10.1038/s41467-019-13907-7.
- (4) Wang, Z.; Jiang, Y.; Jin, F.; Stampfl, C.; Hunger, M.; Baiker, A.; Huang, J. Strongly enhanced acidity and activity of amorphous silica–alumina by formation of pentacoordinated Al^V species. *J. Catal.* **2019**, *372*, 1-7.
- (5) Huang, J.; van Vegten, N.; Jiang, Y.; Hunger, M.; Baiker, A. Increasing the Brønsted acidity of flame-derived silica/alumina up to zeolitic strength. *Angew. Chem. Int. Ed.* **2010**, *49*, 7776-7781.
- (6) Hunger, M.; Freude, D.; Pfeifer, H.; Bremer, H.; Jank, M.; Wendlandt, K. P., High-resolution proton magnetic-resonance and catalytic studies concerning Brønsted centers of amorphous Al₂O₃-SiO₂ solids. *Chem. Phys. Lett.* **1983**, *100*, 29-33.
- (7) Duevel, A.; Romanova, E.; Sharifi, M.; Freude, D.; Wark, M.; Heitjans, P.; Wilkening, M. Mechanically induced phase transformation of gamma-Al₂O₃ into alpha-Al₂O₃. Access to structurally disordered gamma-Al₂O₃ with a controllable amount of pentacoordinated Al sites. *J. Phys. Chem. C* **2011**, *115*, 22770-22780.
- (8) MacKenzie, K. J. D.; Temuujin, J.; Okada, K. Thermal decomposition of mechanically activated gibbsite. *Thermochimica Acta* **1999**, *327*, 103-108.
- (9) Wischert, R.; Laurent, P.; Coperet, C.; Delbecq, F.; Sautet, P. gamma-Alumina: The essential and unexpected role of water for the structure, stability, and reactivity of "defect" sites. *J. Am. Chem. Soc.* **2012**, *134*, 14430-14449.
- (10) Chupas, P. J.; Chapman, K. W.; Halder, G. J. Elucidating the structure of surface acid sites on gamma-Al₂O₃. *J. Am. Chem. Soc.* **2011**, *133*, 8522-8524.

- (11) Deng, H.; Yu, Y.; Liu, F.; Ma, J.; Zhang, Y.; He, H., Nature of Ag species on Ag/gamma-Al₂O₃: A combined experimental and theoretical study. *ACS Catal.* **2014**, *4*, 2776-2784.
- (12) Duan, H.; You, R.; Xu, S.; Li, Z.; Qian, K.; Cao, T.; Huang, W.; Bao, X. Pentacoordinated Al³⁺-stabilized active Pd structures on Al₂O₃-coated palladium catalysts for methane combustion. *Angew. Chem.* **2019**, *131*, 12171–12176.
- (13) Shi, L.; Deng, G.-M.; Li, W. C.; Miao, S.; Wang, Q. N.; Zhang, W. P.; Lu, A. H. Al₂O₃ nanosheets rich in pentacoordinate Al³⁺ ions stabilize Pt-Sn clusters for propane dehydrogenation. *Angew. Chem. Int. Ed.* **2015**, *54*, 13994-13998.
- (14) Chizallet, C.; Raybaud, P. Pseudo-bridging silanols as versatile Brønsted acid sites of amorphous aluminosilicate surfaces. *Angew. Chem. Int. Ed.* **2009**, *48*, 2891-2893.
- (15) Keller, T. C.; Arras, J.; Haus, M. O.; Hauert, R.; Kenvin, A.; Kenvin, J.; Pérez-Ramírez, J. Synthesis-property-performance relationships of amorphous silica-alumina catalysts for the production of methylenedianiline and higher homologues. *J. Catal.* **2016**, *344*, 757-767.
- (16) Mouat, A. R.; George, C.; Kobayashi, T.; Pruski, M.; van Duyne, R. P.; Marks, T. J.; Stair, P. C. Highly dispersed SiO_x/Al₂O₃ catalysts illuminate the reactivity of isolated silanol sites. *Angew. Chem. Int. Ed.* **2015**, *54*, 13346-13351.
- (17) Valla, M.; Rossini, A. J.; Caillot, M.; Chizallet, C.; Raybaud, P.; Digne, M.; Chaumonnot, A.; Lesage, A.; Emsley, L.; van Bokhoven, J. A.; Coperet, C. Atomic description of the interface between silica and alumina in aluminosilicates through dynamic nuclear polarization surface-enhanced NMR spectroscopy and first-principles calculations. *J. Am. Chem. Soc.* **2015**, *137*, 10710-10719.

- (18) Dewitte, B. M.; Grobet, P. J.; Uytterhoeven, J. B. Pentacoordinated aluminum in noncalcined amorphous aluminosilicates, prepared in alkaline and acid-medium. *J. Phys. Chem.* **1995**, *99*, 6961-6965.
- (19) Kwak, J. H.; Hu, J. Z.; Kim, D. H.; Szanyi, J.; Peden, C. H. F. Penta-coordinated Al³⁺ ions as preferential nucleation sites for BaO on gamma-Al₂O₃: An ultra-high-magnetic field Al-27 MAS NMR study. *J. Catal.* **2007**, *251*, 189-194.
- (20) Koirala, R.; Pratsinis, S. E.; Baiker, A. Synthesis of catalytic materials in flames: opportunities and challenges. *Chem. Soc. Rev.* **2016**, *45*, 3053-3068.
- (21) Amoureux, J. P.; Fernandez, C.; Steuernagel, S. Z filtering in MQMAS NMR. *J. Magn. Reson. Ser. A* **1996**, *123*, 116-118.
- (22) Williams, M. F.; Fonfe, B.; Sievers, C.; Abraham, A.; van Bokhoven, J. A.; Jentys, A.; van Veen, J. A. R.; Lercher, J. A. Hydrogenation of tetralin on silica-alumina-supported Pt catalysts I. Physicochemical characterization of the catalytic materials. *J. Catal.* **2007**, *251*, 485-496.
- (23) Wouters, B. H.; Chen, T. H.; Grobet, P. J., Reversible tetrahedral-octahedral framework aluminum transformation in zeolite Y. *J. Am. Chem. Soc.* **1998**, *120*, 11419-11425.
- (24) Omega, A.; van Bokhoven, J. A.; Prins, R., Flexible aluminum coordination in aluminosilicates. Structure of zeolite H-USY and amorphous silica-alumina. *J. Phys. Chem. B* **2003**, *107*, 8854-8860.
- (25) Hunger, M., Solid-State NMR Spectroscopy. In *Zeolite Characterization and Catalysis - A Tutorial*, A.W. Chester, E. G. D., Ed. Springer: Heidelberg, 2009; pp 65-105.
- (26) Xu, J.; Wang, Q.; Deng, F. Metal active sites and their catalytic functions in zeolites: Insights from solid-state NMR spectroscopy. *Acc. Chem. Res.* **2019**, *52*, 2179-2189.

- (27) Zheng, A. M.; Li, S. H.; Liu, S. B.; Deng, F. Acidic properties and structure-activity correlations of solid acid catalysts revealed by solid-state NMR spectroscopy. *Acc. Chem. Res.* **2016**, *49*, 655-663.
- (28) Perras, F. A.; Wang, Z.; Kobayashi, T.; Baiker, A.; Huang, J.; Pruski, M. Shedding light on the atomic-scale structure of amorphous silica-alumina and its Brønsted acid sites. *Phys. Chem. Chem. Phys.* **2019**, *21*, 19529-19537.
- (29) Wang, Z.; Jiang, Y.; Stampfl, C.; Baiker, A.; Hunger, M.; Huang, J. NMR spectroscopic characterization of flame-made amorphous silica-alumina for cyclohexanol and glyceraldehyde conversion. *ChemCatChem* **2020**, *12*, 287-293.
- (30) Wang, Z.; Ling, H.; Shi, J.; Stampfl, C.; Yu, A.; Hunger, M.; Huang, J. Acidity enhanced [Al]MCM-41 via ultrasonic irradiation for the Beckmann rearrangement of cyclohexanone oxime to ϵ -caprolactam. *J. Catal.* **2018**, *358*, 71-79.
- (31) Wang, Z.; Jiang, Y.; Rachwalik, R.; Liu, Z.; Shi, J.; Hunger, M.; Huang, J. One-step room-temperature synthesis of Al-MCM-41 materials for the catalytic conversion of phenylglyoxal to ethylmandelate. *ChemCatChem* **2013**, *5*, 3889-3896.
- (32) Jiang, Y.; Huang, J.; Dai, W.; Hunger, M. Solid-state nuclear magnetic resonance investigations of the nature, property, and activity of acid sites on solid catalysts. *Solid State Nucl. Magn. Reson.* **2011**, *39*, 116-141.
- (33) Li, S.; Zheng, A.; Su, Y.; Zhang, H.; Chen, L.; Yang, J.; Ye, C.; Deng, F., Brønsted/Lewis acid synergy in dealuminated HY zeolite: A combined solid-state NMR and theoretical calculation study. *J. Am. Chem. Soc.* **2007**, *129*, 11161-11171.
- (34) Stebbins, J. F.; Xu, Z. NMR evidence for excess non-bridging oxygen in an aluminosilicate glass. *Nat.* **1997**, *390*, 60-62.

- (35) Huang, J.; Jiang, Y. J.; Marthala, V. R. R.; Ooi, Y. S.; Hunger, M. Regioselective H/D exchange at the side-chain of ethylbenzene on dealuminated zeolite H-Y studied by in situ MAS NMR-UV/Vis spectroscopy. *Chemphyschem* **2008**, *9* (8), 1107-1109.
- (36) Huang, J.; Jiang, Y. J.; Marthala, V. R. R.; Wang, W.; Sulikowski, B.; Hunger, M. In situ H-1 MAS NMR investigations of the H/D exchange of alkylaromatic hydrocarbons on zeolites H-Y, La,Na-Y, and H-ZSM-5. *Microporous Mesoporous Mater.* **2007**, *99*, 86-90.
- (37) Huang, J.; Jiang, Y.; Marthala, V. R. R.; Hunger, M. Insight into the mechanisms of the ethylbenzene disproportionation: Transition state shape selectivity on zeolites. *J. Am. Chem. Soc.* **2008**, *130*, 12642-12644.
- (38) Beck, L. W.; Xu, T.; Nicholas, J. B.; Haw, J. F. Kinetic NMR and density-functional study of benzene H/D exchange in zeolites, the most simple aromatic-substitution. *J. Am. Chem. Soc.* **1995**, *117*, 11594-11595.
- (39) Zeng, X.; Wang, Z.; Ding, J.; Wang, L.; Jiang, Y.; Stampfl, C.; Hunger, M.; Huang, J. Catalytic arene alkylation over H-Beta zeolite: Influence of zeolite shape selectivity and reactant nucleophilicity. *J. Catal.* **2019**, *380*, 9-20.
- (40) Pescarmona, P. P.; Janssen, K. P. F.; Delaet, C.; Stroobants, C.; Houthoofd, K.; Philippaerts, A.; De Jonghe, C.; Paul, J. S.; Jacobs, P. A.; Sels, B. F. Zeolite-catalysed conversion of C(3) sugars to alkyl lactates. *Green Chem.* **2010**, *12*, 1083-1089.
- (41) Corma, A.; Iborra, S.; Velty, A. Chemical routes for the transformation of biomass into chemicals. *Chem. Rev.* **2007**, *107*, 2411-2502.
- (42) Wang, Z.; Jiang, Y.; Baiker, A.; Huang, J. Efficient acid-catalyzed conversion of phenylglyoxal to mandelates on flame-derived silica/alumina. *ACS Catal.* **2013**, *3*, 1573-1577.

- (43) Kim, K. D.; Wang, Z.; Jiang, Y.; Hunger, M.; Huang, J. The cooperative effect of Lewis and Brønsted acid sites on Sn-MCM-41 catalysts for the conversion of 1,3-dihydroxyacetone to ethyl lactate. *Green Chem.* **2019**, *21*, 3383-3393.
- (44) Wang, Z.; Wang, L.; Jiang, Y.; Hunger, M.; Huang, J. Cooperativity of Brønsted and Lewis acid sites on zeolite for glycerol dehydration. *ACS Catal.* **2014**, *4*, 1144-1147.
- (45) Wang, C.; Chu, Y.; Xu, J.; Wang, Q.; Qi, G.; Gao, P.; Zhou, X.; Deng, F. Extra-framework aluminum-assisted initial C–C bond formation in methanol-to-olefins conversion on zeolite H-ZSM-5. *Angew. Chem. Int. Ed.* **2018**, *57*, 10197-10201.
- (46) Wang, Z.; O'Dell, L. A.; Zeng, X.; Liu, C.; Zhao, S.; Zhang, W.; Gaborieau, M.; Jiang, Y.; Huang, J. Insight into Three-Coordinate Aluminum Species on Ethanol-to-Olefin Conversion over ZSM-5 Zeolites. *Angew. Chem. Int. Ed.* **2019**, *58*, 18061-18068.
- (47) Dapsens, P. Y.; Mondelli, C.; Perez-Ramirez, J. Highly selective Lewis acid sites in desilicated MFI zeolites for dihydroxyacetone isomerization to lactic acid. *ChemSusChem* **2013**, *6*, 831-839.
- (48) Moreno-Recio, M.; Santamaria-Gonzalez, J.; Maireles-Torres, P. Brønsted and Lewis acid ZSM-5 zeolites for the catalytic dehydration of glucose into 5-hydroxymethylfurfural. *Chem. Eng. J.* **2016**, *303*, 22-30.
- (49) Xu, B.; Sievers, C.; Lercher, J. A.; van Veen, J. A. R.; Giltay, P.; Prins, R.; van Bokhoven, J. A. Strong Brønsted acidity in amorphous silica–aluminas. *J. Phys. Chem. C* **2007**, *111*, 12075-12079.
- (50) Wang, Z.; Jiang, Y.; Hunger, M.; Baiker, A.; Huang, J. Catalytic performance of Brønsted and Lewis acid sites in phenylglyoxal conversion on flame-derived silica-zirconia. *ChemCatChem* **2014**, *6*, 2970-2975.

(51) Kwak, J. H.; Hu, J.; Mei, D.; Yi, C. W.; Kim, D. H.; Peden, C. H. F.; Allard, L. F.; Szanyi, J. Coordinatively Unsaturated Al³⁺ centers as binding sites for active catalyst phases of platinum on gamma-Al₂O₃. *Sci.* **2009**, *325*, 1670-1673.

(52) Giannakakis, G.; Flytzani-Stephanopoulos, M.; Sykes, E. C. H. Single-Atom alloys as a reductionist approach to the rational design of heterogeneous catalysts. *Acc. Chem. Res.* **2019**, *52*, 237-247.

(53) Liu, L. C.; Corma, A. Metal catalysts for heterogeneous catalysis: From single atoms to nanoclusters and nanoparticles. *Chem. Rev.* **2018**, *118*, 4981-5079.

